Solubilities of AOT Analogues Surfactants in Supercritical CO$_2$ and HFC-134a Fluids

Zhao-Tie Liu,*,† Jin Wu,† Ling Liu,† Changan Sun,† Liping Song,† Ziwei Gao,† Wensheng Dong,† and Jian Lu†,‡

Key Laboratory for Macromolecular Science of Shaanxi Province, School of Chemistry & Materials Science, Shaanxi Normal University, Xi'an, 710062, People's Republic of China, and Xi'an Modern Chemistry Research Institute, Xi'an, 710065, People's Republic of China

A series of sodium bis(2-ethylhexyl) sulfosuccinate (AOT) analogue surfactants [sodium dibutyl sulfosuccinate (DBSS), sodium dipentyl sulfosuccinate (DPSS), sodium dihexyl sulfosuccinate (DHSS), and sodium dioctyl sulfosuccinate (DOSS)] were synthesized and characterized with ^{1}H NMR and elemental analysis. The solubilities of surfactants in supercritical CO$_2$ (scCO$_2$) and supercritical 1,1,1,2-tetrafluoroethane (HFC-134a) fluids at a temperature range from (308 to 338) K and under pressures of (10 to 30) MPa were measured using a static method coupled with gravimetric analysis. The solubilities of these surfactants are much higher in HFC-134a fluid as compared with that in scCO$_2$. The solubilities increased with increasing temperature and pressure for both scCO$_2$ and HFC-134a fluids. The solubilities in scCO$_2$ increased with increasing carbon atom number of surfactant, whereas they decreased with increasing carbon atom number of surfactant in HFC-134a. The density of scCO$_2$ was simulated with the Peng−Robinson (P-R) equation. The experimental data were used to validate the accuracy of the P-R equation.

Introduction

Attributed to the advantages of supercritical fluid (SCF) over conventional liquid solvents (such as its low surface tension, high diffusivity, low viscosity, high compressibility) as well as its density, dielectric constant, diffusion coefficient, and solubility parameter being able to be tuned continuously by changing pressure and temperature, supercritical fluids have become attractive solvents in many industrial processes including extraction,[1] processing of polymer,[2] phase transfer reactions and catalysis,[3] enzymatic catalysis,[4] processing of microelectronic devices,[5] and synthesis of nanoparticals.[6−9]

Supercritical carbon dioxide (scCO$_2$) is the most popular solvent among SCFs due to its nontoxic, nonflammable, inexpensive, easy to obtain, and near-ambient critical temperature. Solubility of pure substances in supercritical CO$_2$ has been reported in recent years.[10−23] However, the solubility of some polar compounds and ionic compounds having high molecular weight in scCO$_2$ is very low, which limits its application in industry.[24] Fortunately, these polar substances can easily dissolve in fluorohydrocarbons such as chlorodifluoromethane (HCFC-22), trifluoromethane (HFC-23), difluoroethane (HFC-32), pentafluoroethane (HFC-125), 1,1,1,2-tetrafluoroethane (HFC-134a), 1,1,1-trifluoroethane (HFC-143a), 1,1-difluoroethane (HFC-152a), 1,1,1,2,3,3,3-heptafluoro-propane (HFC-227ea), and dimethyl ether (DME).[25−32]

Knowledge of the solubility of solids in SCFs is essential for evaluating the feasibility of SCFs application and for establishing optimum conditions of operation. Solubility measurements have therefore received considerable attention.[22,33−35]

Succinate sulfonates (SS) are widely used in many fields such as chemical industry concerned with products for daily use,

paint, dye printing, medicament, agricultural pesticide, mines, paper manufacture, leather making, and photosensitize industry. These surfactants have a prominent property in that the molecular structure can be adjusted to fit into demands of different application fields. Moreover, the synthesis method has a simple production process, a low cost, and a small quantity of pollution. Therefore, the solubility determination of SSs is a very important precondition for surfactant application in SCFs.

Generally, two techniques—flowing method and static method— are used to measure solubilitiy in SCFs. The calculations of solubility are correlated using a mathematical model such as the semiempirical model proposed first by Bartle, which was afterward used successfully by others; the model proposed by Chrastil; and some equations, such as the Peng−Robinson (P-R) and the Soave−Redlich−Kwong (S-R-K) equations.[36−41]

In this study, we consult the method and procedures given by Sherman et al.[23] The static method coupled with gravimetric analysis was used to determine the solubilities of SS surfactants in SCFs. The density of scCO$_2$, depending on pressure and temperature, was also simulated with the P-R equation. The experimental data were used to validate the accuracy of the P-R equation and will provide useful data for our future applications of these surfactants.
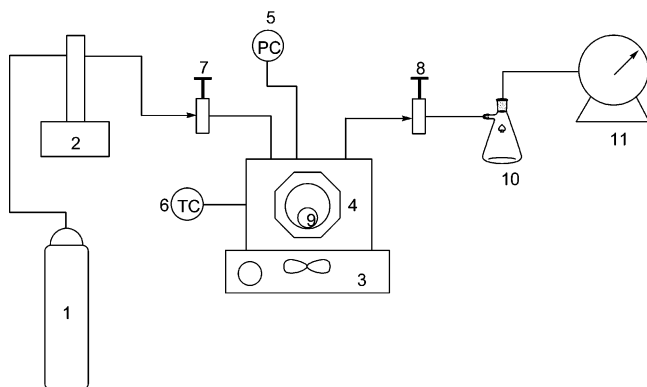
Experimental Section

Materials and Instruments. Maleic anhydride, *p*-toluenesulfonic acid monohydrate (99.0 %), *n*-hexanol (99.0 %), and 1,4-dioxane (99.5 %) were obtained from Sinopharm Group Chemical Reagent Co. Sodium hydrogen sulfite (SO$_2$: 65.0 %), *n*-pentanol (98.0 %), *n*-octanol (99.5 %), ethanol (99.7 %), sodium hydroxide (99.0 %), and toluene (99.5 %) were obtained from Xi'an Chemical Reagent Factory. Acetone-*d*$_6$ (*d*: 99.8 %) was obtained from Beijing Chemical Reagent Factory, *n*-butanol (99.0 %) was taken from Tianjin No. 3 Chemical Reagent Factory, CO$_2$ (99.9 %) was obtained from Xi'an Yatai Liquid Gas

---

* Corresponding author. Fax: +86 29 85303682. E-mail: ztliu@snnu.edu.cn.
† Shaanxi Normal University.
‡ Xi'an Modern Chemistry Research Institute.

Figure 1. Schematic diagram of experimental setup: 1, carbon dioxide cylinder; 2, ISCO model 260D syringe pump; 3, magnetic stir device; 4, SF-400 high-pressure vessel; 5, pressure transducer; 6, thermocouple assembly; 7, intake valve; 8, back pressure valve; 9, sample vial; 10, reclaimer vase; 11, wet-type gas meter.

Co., and 1,1,1,2-tetrafluoroethane (HFC-134a) (99.9 %) was obtained from Xi'an Jinzhu Modern Chemical Industry Co., Ltd. The chemical reagents used in this study were of analytically pure grade.

The schematic diagram of experimental apparatus for solubility measurement is given in Figure 1. The solubility measurement of surfactants in $scCO_2$ and HFC-134a was investigated by using a high-pressure vessel (SF-400, Beijing, Sihe Chuangzhi Keji Corporation) with a maximum pressure of 40 MPa, a maximum temperature of 353 K, and an internal volume of 60 cm.[3] The vessel was equipped with two sapphire windows with a diameter of 25 mm and a thickness of 20 mm. The windows were sealed on both sides with poly(ether−ether−ketone) (PEEK) seals. The ISCO model 260D syringe pump was used to charge CO_2 and HFC-134a fluids into the high-pressure vessel.

The ^{1}H NMR spectra were recorded on a Superconducting Fourier digital NMR spectrometer (Bruker, AVANCF 300MHZ). The elemental analysis of the samples was done by elemental analyzer (Germany, Vario EL III).

Surfactant Synthesis. The modified synthesis procedures of surfactants were conducted according to the methods given by Liu and Erkey.[42] The surfactants of sodium dibutyl sulfosuccinate, sodium dipentyl sulfosuccinate, sodium dihexyl sulfosuccinate, and sodium dioctyl sulfosuccinate were synthesized in an unclosed system and without any extra phase transfer catalyst. The process was carried out by esterification and sulfonation reactions.

A mixture of maleic anhydride, hydrocarbon alcohol, and *p*-toluenesulfonic acid monohydrate as catalyst was refluxed under stirring; liberated water was removed azeotropically from the reaction system to shift equilibrium of esterification. Water created in this reaction was collected in the trap. The reaction was stopped when about 94 % of the theoretical amount of water was collected in the trap. Subsequently, the esterifiable product was neutralized to pH 7 by using aqueous sodium hydroxide (30 %), and floc were observed in the system. Then an aqueous sodium hydrogen sulfite in distilled water and ethanol as cosolvent were added into the system. The mixture was refluxed under stirring at a fixed temperature for several hours. The reaction was stopped if no oily matter floated on the water surface, and the pH of the reaction system was neutral. A white solid was obtained after purification, recrystallization, and drying at 313 K under vacuum overnight.

The surfactants were characterized with ^{1}H NMR spectroscopy and elemental analysis as follows.
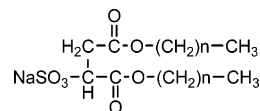
Figure 2. Surfactants synthesized and used in this study. (1) DBSS: $n = 3$, sodium dibutyl sulfosuccinate. (2) DPSS: $n = 4$, sodium dipentyl sulfosuccinate. (3) DHSS: $n = 5$, sodium dihexyl sulfosuccinate. (4) DOSS: $n = 7$, sodium dioctyl sulfosuccinate.

(1) Sodium dibutyl sulfosuccinate. $CH_3^aCH_2^bCH_2^cCH_2^dOO$-$CCH_2^eCH^f(SO_3Na)COOCH_2^gCH_2^hCH_2^iCH_3^j$ (yield, 90.4 %). ^{1}H NMR ($CDCl_3$, δ): 0.93 (a and j, t, $J = 2.96$ Hz, 6H), 1.36 (b and i, t, $J = 7.68$ Hz, 4H), 1.58 (c and h, t, $J = 7.55$ Hz, 4H), 3.18 (e, t, $J = 9.64$ Hz, 2H), 4.05 (d, t, $J = 6.73$ Hz, 2H), 4.18 (g, t, $J = 6.56$ Hz, 2H), 4.33 (f, t, $J = 5.12$ Hz, 1H). Anal. Calcd: C, 43.37; S, 9.65; H, 6.37. Found: C, 43.31; S, 10.07; H, 6.41.

(2) Sodium dipentyl sulfosuccinate. $CH_3^aCH_2^bCH_2^cCH_2^dCH_2^e$-$OOCCH_2^fCH^g(SO_3Na)COOCH_2^hCH_2^iCH_2^jCH_2^kCH_3^l$ (yield, 95.1 %). ^{1}H NMR ($CDCl_3$, δ): 0.91−0.87 (a and l, t, $J = 3.70$ Hz, 6H), 1.30−1.35 (b, c, j, and k, m, $J = 3.09$ Hz, 8H), 1.67−1.55 (d and i, m, $J = 6.89$ Hz, 4H), 3.23−3.08 (f, m, $J = 11.76$ Hz, 2H), 4.04 (e, t, $J = 6.84$ Hz, 2H), 4.14−4.18 (h, m, $J = 5.05$ Hz, 2H), 4.26−4.31 (g, m, $J = 4.95$ Hz, 1H). Anal. Calcd: C, 46.65; S, 8.90; H, 6.99. Found: C, 46.14; S, 8.42; H, 6.71.

(3) Sodium dihexyl sulfosuccinate. $CH_3^aCH_2^bCH_2^cCH_2^d$-$CH_2^eCH_2^fOOCCH_2^gCH^h(SO_3Na)COOCH_2^iCH_2^jCH_2^kCH_2^lCH_2^m$-$CH_3^n$ (yield, 84.7 %). ^{1}H NMR ($CDCl_3$, δ): 0.90 (a and n, t, $J = 4.59$ Hz, 6H), 1.29 (b, c, d, k, l, and m, t, $J = 1.38$ Hz, 8H), 1.59 (e and j, t, $J = 6.87$ Hz, 4H), 3.15 (g, t, $J = 9.33$ Hz, 2H), 4.05 (f, t, $J = 6.87$ Hz, 2H), 4.14 (i, t, $J = 6.6$ Hz, 2H), 4.33 (h, t, $J = 5.16$ Hz, 1H). Anal. Calcd: C, 49.47; S, 8.25; H, 7.52. Found: C, 49.57; S, 8.22; H, 7.41.

(4) Sodium dioctyl sulfosuccinate. $CH_3^aCH_2^bCH_2^cCH_2^dCH_2^e$-$CH_2^fCH_2^gCH_2^hOOCCH_2^iCH^j(SO_3Na)COOCH_2^kCH_2^lCH_2^mCH_2^n$-$CH_2^oCH_2^p CH_2^qCH_3^r$ (yield, 86.6 %). ^{1}H NMR ($CDCl_3$, δ): 0.88 (a and r, t, $J = 6.75$ Hz, 6H), 1.27 (b, c, d, e, f, m, n, o, p, and q, m, $J = 12.84$ Hz, 20H), 1.59 (g and l, m, $J = 5.76$ Hz, 4H), 3.14−3.17 (i, m, $J = 4.57$ Hz, 2H), 4.02 (h, t, $J = 6.87$ Hz, 2H), 4.13−4.18 (k, m, $J = 6.51$ Hz, 2H), 4.27−4.32 (j, m, $J = 4.04$, 1H). Anal. Calcd: C, 54.03; S, 7.21; H, 8.39. Found: C, 54.97; S, 6.99; H, 8.33.

Solubility Measurement. The structures of surfactants synthesized and used to measure solubility are listed in Figure 2. A variety of methods have been developed to measure the solubility of solutes in $scCO_2$, which can be classified as dynamic or static methods. In the dynamic methods, the solute is loaded into a high pressure extraction vessel that is continuously swept with $scCO_2$, and the solubility is calculated from an analysis of the solute concentration in the effluent stream. The static methods may be divided into two categories on the basis of the type of vessel used. A variable-volume view cell enables one to determine the solubility by visual inspection of a cloud point. The use of a fixed-volume cell requires an analysis of the fluid phase to determine the solubility. Alternatively, one can couple a fixed volume cell with a suitable high-pressure spectroscopic method that directly measures the solute concentrations in the fluid phase. However, high-pressure absorption spectroscopy requires special equipment that is usually very expensive. Sherman et al.[23] reported a simple static method using a fixed-volume vessel combined with gravimetric analysis for determining the solubility of solids in $scCO_2$.

The solubility of these surfactants was measured by modification of the procedures given by Sherman et al.[23] In the process of solubility measurement, an excess amount of surfactant and a small magnetic stir bar were packed in a 12 mL (25 mm ×

25 mm) glass vial that was then capped with coarse filter paper attached to the vial with Teflon tape. A larger stir magnetic stir bar was placed inside the high-pressure vessel. The high-pressure vessel was sealed, placed on a magnetic stirrer plate, and heated to the desired temperature by a controllable heater. Once it reached the desired temperature, stirring was initiated, and the vessel was slowly filled with CO_2 or HFC-134a until the desired pressure was achieved. After sufficient time was allowed for equilibration of CO_2/solute or HFC-134a/solute solution, the vessel was depressurized and opened. The surfactants were reclaimed at the end of experimentation. The vial was removed, wiped with a clean tissue, dried, and reweighed. The solubilities of surfactants in SCFs are calculated by the P-R equation in our work and the equation given by Sherman et al. (eq 1).[23] The solubility of surfactant in supercritical fluids is given as

$$solubility = (M_1 - M_2)/(V_1 - V_2) \qquad (1)$$

where M_1 and M_2 are the initial and final measured mass of solute in the vial, V_1 is the volume of the high-pressure vessel, and V_2 is the volume of vial. This equation incorporates a correction factor that accounts for precipitation of the solute in the fluid phase in the vial. The volume of the vessel in eq 1 is the volume accessible to the fluid phase, which was determined as 48 mL.

Foundation of P-R Equation. Although it has obvious disadvantages, the P-R equation possesses appropriate qualitative description and superior accuracy of quantitative calculation for the phase behavior of SCFs. The P-R equation can apply to many complicated systems, which were comprised with SCFs.

The standard form of the P-R equation[41,43] is given by

$$P = \frac{RT}{V - b} - \frac{a}{V(V + b) + b(V - b)} \qquad (2)$$

Expand the P-R equation to the cubic equation of V:

$$V^3 - \left(\frac{RT}{P} - b\right)V^2 + \left(\frac{a}{P} - \frac{2bRT}{P} - 3b^2\right)V - \\ \left(\frac{ab}{P} - RTb^2 - b^3\right) = 0 \quad (3)$$

because

$$Z = \frac{PV}{RT} \quad V = \frac{ZRT}{P} \qquad (4)$$

Take eq 4 to eq 3, then the cubic equation of Z is obtained:

$$Z^3 - \left(1 - \frac{bP}{RT}\right)Z^2 + \left(\frac{aP}{R^2T^2} - 2\frac{bP}{RT} - 3\frac{b^2P^2}{R^2T^2}\right)Z - \\ \left(\frac{aP}{R^2T^2} \times \frac{bP}{RT} - \frac{b^2P^2}{R^2T^2} - \frac{b^3P^3}{R^3T^3}\right) = 0 \quad (5)$$

Suppose

$$A = \frac{ap}{R^2T^2} \quad B = \frac{bp}{RT} \qquad (6)$$

The compressed factor can be assigned as

$$Z^3 - (1 - B)Z^2 + (A - 2B - 3B^2)Z - (AB - B^2 - B^3) = 0 \quad (7)$$

The density of CO_2 is formulated as

$$\rho = \frac{PM}{ZRT} \qquad (8)$$

where

$$A = \frac{ap}{R^2T^2} \quad B = \frac{bp}{RT}$$

$$a = a_c \times \alpha = 0.457235\frac{R^2T_c^{\,2}}{p_c}\alpha$$

$$b = 0.077796\frac{RT_c}{p_c}$$

$$\alpha^{0.5} = 1 + m(1 - T_r^{0.5})$$

$$m = 0.37646 + 1.54226\omega - 0.26992\omega^2$$

$$T_r = \frac{T}{T_c}$$

where ω is the eccentric factor, T_c is the critical temperature, P_c is *the* critical pressure, and T_r is the contrastive temperature. Then the solution of cubic equation of Z is worked out. Take the calculated solution of Z to the equation of $\rho = PM/ZRT$, and the density of CO_2 is obtained.

Measurement and Calculation of Pure CO_2 Density. The calculation methods of pure CO_2 density for measurement system are listed from eq 9 to eq 15. The relationship between the factor and the density of CO_2 can be represented by the ideal gas-state equation:

$$PV = nRT \qquad (9)$$

where P is the ideal state pressure (0.101325 MPa), V is the ideal state volume of CO_2, T is the ideal state temperature (273.15 K), and n and R are constants.

As we know that

$$\frac{P_1V_1}{T_1} = \frac{PV}{T} \qquad (10)$$

where P_1 is the room pressure of the experiment, V_1 is the volume of CO_2 obtained from the wet-type gas meter, and T_1 is the room temperature of the experiment.

The volume of CO_2 at ideal state can be described as eq 11 on the basis of eq 10:

$$V = \frac{P_1V_1T}{T_1P} \qquad (11)$$

Then the molar of CO_2 is given by

$$n_{CO_2} = \frac{V}{22.4} \qquad (12)$$

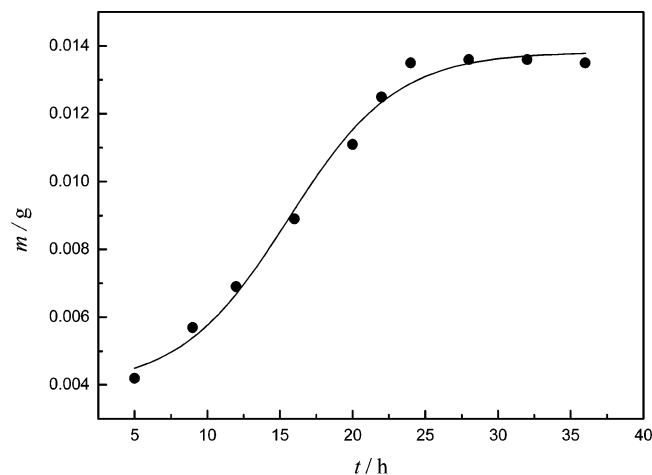where n is the molar of CO_2.

The mass of CO_2 can be calculated by

$$m_{CO_2} = M_{CO_2} \times n_{CO_2} \qquad (13)$$

where m is the mass of CO_2 in the high-pressure vessel, and M is the molar weight of CO_2. The density of CO_2 (ρ) in high-pressure vessel is formulated as
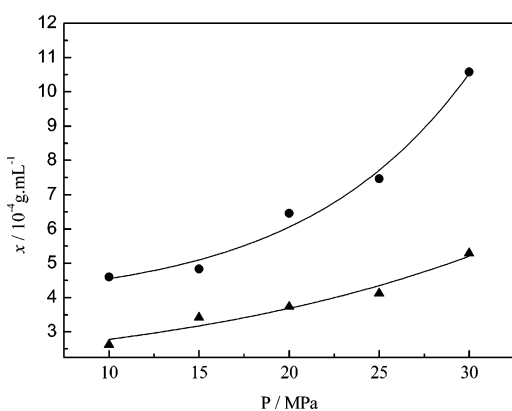
$$\rho = \frac{m_{CO_2}}{V_{vessel}} \qquad (14)$$

or

$$\rho = \frac{n_{CO_2}}{V_{vessel}} \qquad (15)$$

Figure 3. Approach to equilibrium for surfactant/scCO$_2$ system at 308 K and under 10 MPa (m, the amount dissolved; t, equilibrium time).

Figure 4. Solubility (x) of DBSS and DHSS in scCO$_2$ at 318 K and under different pressure: ▲, DBSS; ●, DHSS.

Figure 5. Solubility (x) of DBSS and DHSS in HFC-134a at 318 K and under different pressure: ▲, DBSS; ●, DHSS.

Figure 6. Solubility (x) of DBSS and DHSS in scCO$_2$ under 25 MPa and at different temperature: ▲, DBSS; ●, DHSS.
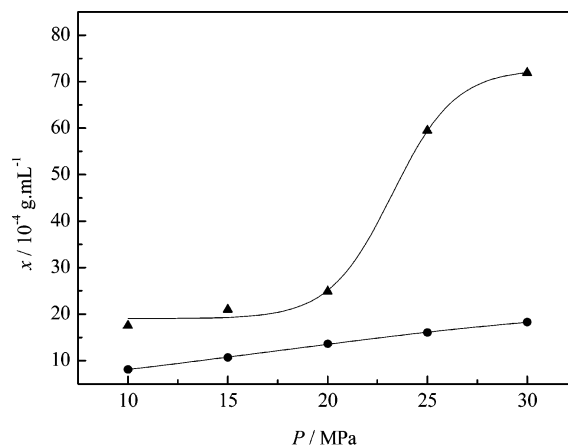
The schematic diagram of the experimental apparatus for CO$_2$ density measurement is the same with that for solubility measurement with the exception that there is the sample vial placed in the high-pressure vessel when measuring the solubility.

The vessel was sealed without any substance, then placed on the magnetic stir plate, and heated to the desired temperature by a controllable heater. The vessel was charged with CO$_2$ from an ISCO syringe pump (model 260D) equipped with a cooling jacket. The pump was stopped when the desired pressure was obtained. When the CO$_2$ in the high-pressure vessel reached to equilibrium, the intake valve was closed, and the back pressure valve was opened to deflate slowly. The volume of CO$_2$ flowing from the wet-type gas meter and the air pressure of aneroid barometer were recorded. The CO$_2$ density was then calculated using eq 9 to eq 15.
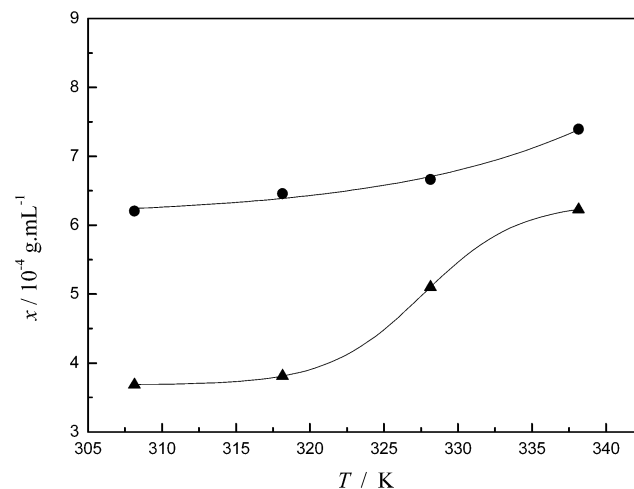
Results and Discussion

Solubility Measurement. The method given by Sherman et al.[23] is used to calculate the solubilities of surfactants in this work. The first set was conducted to determine the time necessary for achieving equilibrium in this solubility measurement system. The solubility of sodium dibutyl sulfosuccinate in scCO$_2$ was determined by the method described in the Experimental Section. The mass of solute lost from the vial is plotted against time in Figure 3 for sodium dibutyl sulfosuccinate in scCO$_2$ at 308 K and under 10 MPa. The CO$_2$ phase became saturated with sodium dibutyl sulfosuccinate after about 24 h.

The solubility data of sodium dibutyl sulfosuccinate and sodium dihexyl sulfosuccinate in scCO$_2$ at 318 K and under

different pressures are shown in Figure 4. The reproducibility for all data obtained in this work was within 5.2 % when the pressure was varied from (10 to 30) MPa. This indicated that the sampling procedure was consistent. Results show that when above the critical pressure of CO$_2$, the solubilities of surfactants increase with increasing pressure. The reason is that, with the pressure increasing, there is a rapid increase in CO$_2$ density. Because the solution power of solvent is proportional to its density, the solution power increased, and the solubility of surfactants in CO$_2$ increases.

The solubilities of sodium dibutyl sulfosuccinate and sodium dihexyl sulfosuccinate in HFC-134a at a fixed temperature and under different pressures are given in Figure 5. The solubility increased with increasing pressure from (10 to 30) MPa at the temperature of 318 K, which is consistent with the results obtained from CO$_2$ as shown in Figure 4. However, the solubilities decreased with increasing carbon atom number of surfactant in HFC-134a, while the solubilities increased with increasing carbon atom number of surfactant in scCO$_2$. Considering these surfactants used, the polarity of molecular decreased with the carbon atom number of the molecular increasing. Because CO$_2$ is a nonpolar solvent, according to the similarity and consistent principle, the surfactant having a higher carbon atom number will give higher solubility in scCO$_2$. HFC-134a is a polar solvent, and thus the surfactant having a higher carbon atom number will give lower solubility in it.

The solubility data of sodium dibutyl sulfosuccinate and sodium dihexyl sulfosuccinate in scCO$_2$ under 25 MPa and at
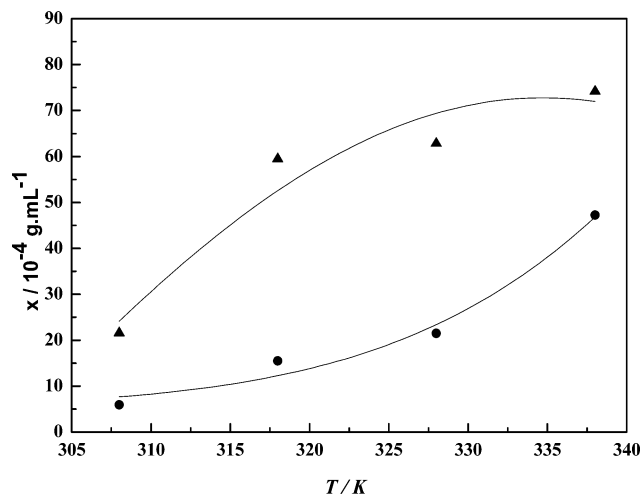
Figure 7. Solubility (x) of DBSS and DHSS in HFC-134a under 25 MPa and at different temperature: ▲, DBSS; ●, DHSS.
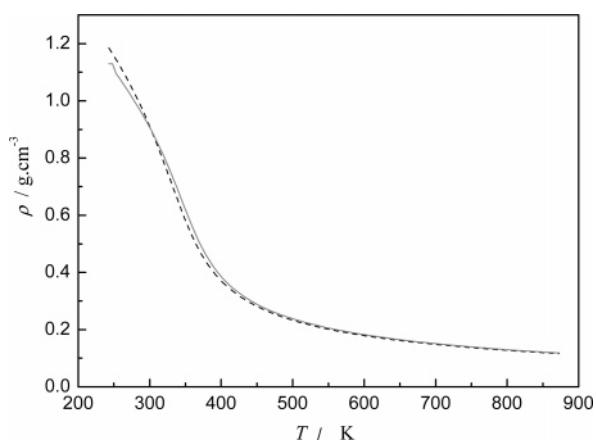
Figure 8. Effect of temperature on theoretical density (ρ) of CO_2 and density (ρ) calculated by P-R equation under 20 MPa: —, theoretical density; - - -, P-R equation.

Table 1. Experimental Solubility Data of Different Surfactants in scCO$_2$ and HFC-134a under 30 MPa and at 318 K[a]

			m/g		$x/10^{-4}$ g·mL^{-1}	
P/MPa	*T*/K	surfactant	CO_2	HFC-134a	CO_2	HFC-134a
		DBSS	0.0254	0.3691	5.292	76.86
30	318	DPSS	0.0301	0.0898	6.271	18.71
		DHSS	0.0353	0.0761	7.354	15.85
		DOSS	0.0463	0.0501	9.646	10.44

[a] *m*, amount dissolved of surfactant; *x*, solubility.

different temperatures are illustrated in Figure 6. The conducted temperature is ranging from (308 to 338) K. The solubility increased with increasing temperature because the decrease in CO_2 density cannot overcome the increase in vapor pressure.

The solubility data of sodium dibutyl sulfosuccinate and sodium dihexyl sulfosuccinate in HFC-134a under a fixed pressure and at different temperatures are shown in Figure 7. The solubility increased with increasing temperature under 25 MPa for both sodium dibutyl sulfosuccinate and sodium dihexyl sulfosuccinate. That is because when the temperature increases, as compared with the decrease of density, the increase of vapor pressure is the most important effect factor. Thus, the solubility of surfactant increased with increasing temperature. This explanation can be used for both CO_2 and HFC-134a solvents.

The solubilities of different surfactants in scCO$_2$ and HFC-134a at the same temperature and pressure are listed in Table
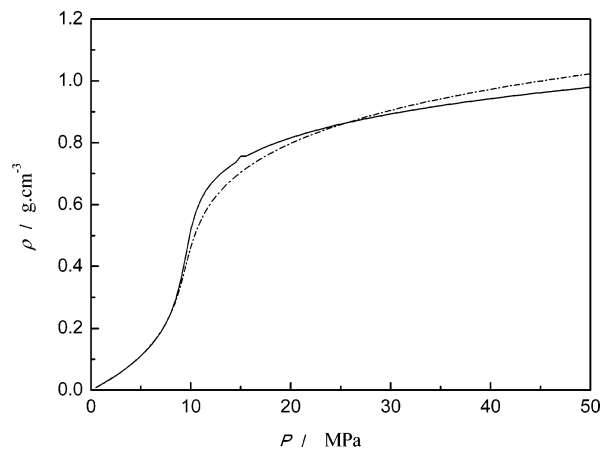
Figure 9. Effect of pressure on theoretical density (ρ) of CO_2 and density (ρ) calculated by P-R equation at 318 K: —, theoretical density; - - -, P-R equation.

1. At the same condition, the solubility of the same surfactant in HFC-134a is much higher as compared with that in scCO$_2$. The results indicate that HFC-134a is a more polar solvent as compared with scCO$_2$ for dissolving the polar compounds. Because CO_2 is a nonpolar solvent with weak van der Waals force, and between solute and CO_2, there exist dipole−quadrupole acting forces that make against the solute dissolving into the solvent. Therefore, polar solutes cannot easily dissolve into CO_2. However, HFC-134a is a polar solvent that has strong solvency to polar solute. Since the dipole−dipole acting force existing between solute and HFC-134a promotes the solute dissolving into the solvent, the solubility of surfactants in HFC-134a is higher as compared with that in scCO$_2$.

Model Analysis. The theoretical results were calculated using a 52-parameter equation of state given by IUPAC.[44] The theoretical density of scCO$_2$ is the approximation of scCO$_2$ density calculated by the P-R equation under 20 MPa and temperature of (273 to 873) K as shown in Figure 8. The distinction of theoretical density of scCO$_2$ (ρ) and the scCO$_2$ density (ρ) calculated by the P-R equation at 318 K under different pressure is shown in Figure 9.

Weng et al.,[45] Yakoumis et al.,[46] and Vieira de Melo et al.[47] give the average absolute error between experimental and calculated concentration of different solutes in scCO$_2$ as shown in eq 16:

$$|\Delta y| = \frac{100}{N}\sum_{i=1}^{N}|y_2^{\text{calc}} - y_2^{\text{exp}}|_i \qquad (16)$$

Caballero et al.[48] defined a percentage average error (% Averr) to express the accuracy of cubic equations of state to correlate experimental phase equilibrium data of several solid−gas systems as shown in eq 17:

$$\% \text{ Averr} = \frac{100\sqrt{\dfrac{1}{N}\sum_{i=1}^{N}[y_2^{\text{calc}} - y_2^{\text{exp}}]_i^2}}{\dfrac{1}{N}\sum_{i=1}^{N}[y_2^{\text{exp}}]_i} \qquad (17)$$

However, Valderrama and Alvarez[49] believe that a true way of expressing the difference between experimental and calculated values is the average percent deviation, expressed in relative form and absolute form as follows:

$$\Delta y_2 \% = \frac{100}{N}\sum_{i=1}^{N}\left[\frac{y_2^{\text{calc}} - y_2^{\text{exp}}}{y_2^{\text{exp}}}\right]_i \qquad (18)$$

$$|\Delta y_2 \%| = \frac{100}{N}\sum_{i=1}^{N}\left[\frac{|y_2^{\text{calc}} - y_2^{\text{exp}}|}{y_2^{\text{exp}}}\right]_i \qquad (19)$$

In the above equations only when $y_2 = 0$, which is a situation of no-interest at all, a different definition is required because eqs 18 and 19 become undetermined. Of the above definitions, the relative deviation without absolute values (eq 18) clearly expresses the true positive and negative deviations of the calculated values with respect to the values of the experimental data. If this relative deviation is zero or close to zero, then this means that positive and negative deviations cancel, but it does not give any indication about how big are those deviations. If the absolute average deviation is small, this means that deviations are also small but we do not know if they are positive or negative. However, if these two deviations are known, then a clear conclusion about the accuracy of given model can be drawn.[49]

Also generalized correlation coefficients and standard deviations may be used to assess statistical goodness of fit or compatibility between experimental data and model results. However, from the practical point of view, the average percent deviation, expressed in relative form and absolute form (eqs 18 and 19), should be used to draw conclusions about how accurate is a set of equation of state, mixing rules, and combining rules to correlate or predict a phase equilibrium variable, such as pressure or gas-phase concentration. This is of special importance for applications such as thermodynamic consistency tests to high-pressure data, cases in which an accurate model to correlate the gas-phase solute concentration is required.[50]

The equations used to calculate standard deviation (s) and absolute error (d) are given as follows:

$$s/\text{g·cm}^{-3} = \sqrt{\frac{(x - \bar{x})^2}{n - 1}} \qquad (20)$$

$$d/\text{g·cm}^{-3} = x - \bar{x} \qquad (21)$$

where $n - 1$ is the degree of freedom.

Figure 10. Density (ρ) calculated by P-R equation and the density (ρ) measured in our work under 20 MPa and at different temperatures: ▲, experimental data; ●, P-R equation data.

The density data of the P-R equation and the density data measured in our work under 20 MPa and at different temperatures are given in Figure 10. It is found that at the same pressure the density curve of the P-R equation is nearly parallel to the density curve measured in our work. The analysis of these data is shown in Table 2. The standard deviation of density measured in our work is 0.0703 g·cm^{-1}, and the standard deviation of the density calculated by the P-R equation is 0.0821 g·cm^{-1}. The two standard deviations are very adjacent, which indicate that the P-R equation is accurate for being used in our experimental calculation.

Further analysis as given in average percent deviation and the absolute percent deviation (Table 2) shows that the density calculated by the P-R equation and the density measured in our work under 20 MPa and at different temperatures has an average percent deviation of -3.63 % and an absolute percent deviation of 3.63 %, which means that a negative 3.63 % conclusion about the accuracy of the P-R model used in this work, while the true absolute percent deviation is 3.63 %.

The density of the P-R equation and the density measured in our work at 318 K and under different pressure are shown in

Table 2. Standard Deviation and Absolute Error of Density Calculated by P-R Equation and Density Measured in Our Work under 20 MPa and at Different Temperatures[a]
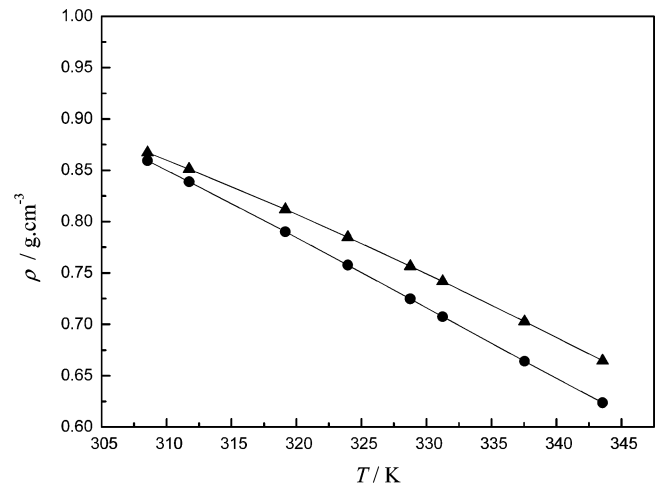
T/K	ρ_1/g·cm^{-3}	ρ_2/g·cm^{-3}	d_1/g·cm^{-3}	d_2/g·cm^{-3}	s_1/g·cm^{-3}	s_2/g·cm^{-3}	Δy_2 %	$\|\Delta y_2 \%\|$
308.4	0.8674	0.8593	0.0948	0.1136				
311.6	0.8512	0.8389	0.0786	0.0932				
319.0	0.8118	0.7902	0.0392	0.0445				
323.8	0.7847	0.7577	0.0121	0.0120				
328.6	0.7566	0.7247	−0.0160	−0.0210	0.0703	0.0821	−3.6264	3.6264
331.1	0.7418	0.7074	−0.0308	−0.0383				
337.4	0.7027	0.6640	−0.0699	−0.0817				
343.4	0.6645	0.6235	−0.1081	−0.1222				

[a] ρ_1, density of our work; ρ_2, density of P-R equation; d_1, absolute error of our work; d_2, absolute error of P-R equation; s_1, standard deviation of our work; s_2, standard deviation of P-R equation.
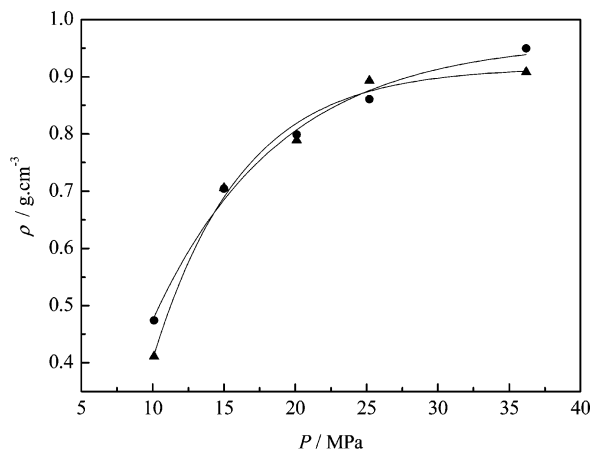
Table 3. Standard Deviation and Absolute Error of Density Calculated by P-R Equation and Density Measured in Our Work at 318 K and under Different Pressures[a]

P/MPa	ρ_1/g·cm^{-3}	ρ_2/g·cm^{-3}	d_1/g·cm^{-3}	d_2/g·cm^{-3}	s_1/g·cm^{-3}	s_2/g·cm^{-3}	Δy_2 %	$\|\Delta y_2 \%\|$
10.1	0.4111	0.4739	−0.3302	−0.2836				
15.0	0.7054	0.7043	−0.0359	−0.0532				
20.1	0.7891	0.7990	0.0478	0.0415	0.2021	0.1820	3.4600	4.9132
25.2	0.893	0.8606	0.1517	0.1031				
36.2	0.9081	0.9495	0.1668	0.1920				

[a] ρ_1, density of our work; ρ_2, density of P-R equation; d_1, absolute error of our work; d_2, absolute error of P-R equation; s_1, standard deviation of our work; s_2, standard deviation of P-R equation.

Figure 11. Density (ρ) calculated by P-R equation and the density (ρ) measured in our work at 318 K and under different pressures: ▲, experimental data; ●, P-R equation data.

Table 4. Molar Fraction (y) of Sodium Dibutyl Sulfosuccinate and Sodium Dihexyl Sulfosuccinate in scCO₂ under 25 MPa and at Different Temperatures[a]

	25 MPa				
	$m/10^{-5}$ mol			$y/10^{-5}$ mol·mol$_{CO_2}{}^{-1}$	
T/K	DBSS	DHSS	M_{CO_2}/mol	DBSS	DHSS
308	5.3257	7.4398	0.9840	5.4123	7.5608
318	5.5062	7.9804	0.9360	5.8827	8.5261
328	7.3717	8.2379	0.8784	8.3922	9.3783
338	8.9965	9.1389	0.8352	10.772	10.942

[a] m, amount dissolved of surfactant; y, mole fraction solubility; M, mole of CO_2.

Figure 11. The curve of density measured in our work is tended toward the curve of density calculated by the P-R equation when the pressure is lower than 25 MPa. The two curves deviated from each other gradually when the pressure was higher than 25 MPa. The analysis of the density data is shown in Table 3. The standard deviation of density obtained in our work is 0.2021 g·cm^{-1}. The standard deviation of density calculated by the P-R equation is 0.1802 g·cm^{-1}.

The analysis as given in average percent deviation and the absolute percent deviation (Table 3) shows that the density calculated by the P-R equation and the density measured in our work at 318 K and under different pressures with an average percent deviation of 3.46 % and an absolute percent deviation of 4.91 %, which mean that a positive 3.46 % conclusion about the accuracy of the P-R model used in this work, while the true absolute percent deviation is 4.91 %.

The molar fraction solubility (y) of sodium dibutyl sulfosuccinate and sodium dihexyl sulfosuccinate in scCO₂ under 25 MPa increases with increasing temperature as listed in Table 4.

Conclusions

The AOT analogues surfactants were synthesized in an unclosed system and without any extra phase transfer catalyst. The solubilities of these surfactants were measured by a static method coupled with gravimetric analysis in scCO₂ and HFC-134a. The solubilities increase with increasing temperature and pressure at the same condition for scCO₂ and HFC-134a. The solubilities of these surfactants in HFC-134a are much higher than that in scCO₂. The solubility of these surfactants is strongly relative to surfactant structure and property of fluid used.

The CO₂ density calculated by the P-R equation and obtained by the theoretical method are close to the experimental results obtained in this work at a wide range of temperatures and pressures investigated. It has been shown that a correct way for analyzing the accuracy of the EoS and the mixing rules are the relative and absolute percent deviations.

Literature Cited

(1) Eckert, C. A.; Knutson, B. L.; Debenedetti, P. G. Supercritical fluids as solvents for chemical and materials processing. *Nature* **1996**, *383*, 313−318.

(2) Cooper, A. I. Polymer synthesis and processing using supercritical carbon dioxide. *J. Mater. Chem.* **2000**, *10*, 207−234.

(3) Dillow, A. K.; Yun, S. L.; Suleiman, D. S.; Boatright, D. L.; Liotta, C. L.; Eckert, C. A. Kinetics of a phase-transfer catalysis reaction in supercritical fluid carbon dioxide. *Ind. Eng. Chem. Res.* **1996**, *35*, 1801−1806.

(4) Holmes, J. D.; Steytler, D. C.; Rees, G. D.; Robinson, B. H. Bioconversions in a water-in-CO₂ microemulsion. *Langmuir* **1998**, *14*, 6371−6376.

(5) Sundararajan, N.; Yang, S.; Ogino, K.; Valiyaveettil, S.; Wang, J.; Zhou, X.; Ober, C. K.; Obendorf, S. K.; Allen, R. D. Supercritical CO₂ processing for submicron imaging of fluoropolymers. *Chem. Mater.* **2000**, *12*, 41−48.

(6) Ji, M.; Chen, X.; Wai, C. M.; Fulton, J. L. Synthesizing and dispersing silver nanoparticles in a water-in-supercritical carbon dioxide microemulsion. *J. Am. Chem. Soc.* **1999**, *121*, 2631−2632.

(7) Ohde, H.; Ohde, M.; Bailey, F.; Kim, H.; Wai, C. M. Water-in-CO₂ microemulsions as nanoreactors for synthesizing CdS and ZnS nanoparticles in supercritical CO₂. *Nano Lett.* **2002**, *2*, 721−724.

(8) Ohde, H.; Rodriguez, J. M.; Ye, X. R.; Wai, C. M. Synthesizing silver halide nanoparticles in supercritical carbon dioxide utilizing a water-in-CO₂ microemulsion. *Chem. Commun.* **2000**, *23*, 2353−2354.

(9) Dong, X.; Potter, D.; Erkey, C. Synthesis of CuS Nanoparticles in water-in-carbon dioxide microemulsions. *Ind. Eng. Chem. Res.* **2002**, *41*, 4489−4493.

(10) Gamse, T.; Steinkellner, F.; Marr, R.; Alessi, P.; Kikic, I. Solubility studies of organic flame retardants in supercritical CO₂. *Ind. Eng. Chem. Res.* **2000**, *39*, 4888−4890.

(11) Mishima, K.; Matsuyama, K.; Baba, M. Solubilities of undecanolide and pentadecanolactone in supercritical carbon dioxide. *J. Chem. Eng. Data* **2001**, *46*, 69−72.

(12) Lee, L. S.; Fu, J. H.; Hsu, H. L. Solubility of solid 1,4-dimethoxy-benzene in supercritical carbon dioxide. *J. Chem. Eng. Data* **2000**, *45*, 358−361.

(13) Xing, H.; Yang, Y. W.; Su, B. G.; Huang, M.; Ren, Q. L. Solubility of artemisinin in supercritical carbon dioxide. *J. Chem. Eng. Data* **2003**, *48*, 330−332.

(14) Ren, Q. L.; Su, B. G.; Huang, M.; Wu, P. D. Solubility of Troeger's base in supercritical carbon dioxide. *J. Chem. Eng. Data* **2000**, *45*, 464−466.

(15) Sovova, H. Solubility of ferulic acid in supercritical carbon dioxide with ethanol as cosolvent. *J. Chem. Eng. Data* **2001**, *46*, 1255−1257.

(16) Sun, Y. Y.; Li, S. F.; Quan, C. Solubility of ferulic acid and tetramethylpyrazine in supercritical carbon dioxide. *J. Chem. Eng. Data* **2005**, *50*, 1125−1128.

(17) Murga, R.; Sanz, M. T.; Beltran, S.; Cabezas, J. L. Solubility of syringic and vanillic acids in supercritical carbon dioxide. *J. Chem. Eng. Data* **2004**, *49*, 779−782.

(18) Asghari, K. M.; Yamini, Y. Solubility of the drugs bisacodyl, methimazole, methylparaben, iodoquinol in supercritical carbon dioxide. *J. Chem. Eng. Data* **2003**, *48*, 61−65.

(19) Liu, J. C.; Han, B. X.; Wang, Z. W.; Zhang, J. L.; Li, G. Z.; Yang, G. Y. Solubility of Ls-36 and Ls-45 surfactants in supercritical CO₂ and loading water in the CO₂/water/surfactant systems. *Langmuir* **2002**, *18*, 3086−3089.

(20) Khosravi, D. K.; Vasheghan, F. E.; Yamini, Y.; Bahramifar, N. Solubility of poly(α-hydroxybutyrate) in supercritical carbon dioxide. *J. Chem. Eng. Data* **2003**, *48*, 860−863.

(21) Morante, E. J.; Suleiman, D.; Este'vez, L. A. Solubilities of imipramine HCl in supercritical carbon dioxide. *Ind. Eng. Chem. Res.* **2003**, *42*, 1821−1823.

(22) Mendez, S. J.; Teja, A. S. Solubility of solids in supercritical fluids: consistency of data and a new model for cosolvent systems. *Ind. Eng. Chem. Res.* **2000**, *39*, 4767−4771.

(23) Sherman, G.; Shenoy, S.; Weiss, R. A. Erkey, C. A static method coupled with gravimetric analysis for the determination of solubilities of solids in supercritical carbon dioxide. *Ind. Eng. Chem. Res.* **2000**, *39*, 846−848.

(24) Consan, K. A.; Smith, R. D. Observations on the solubility of surfactants and related molecules in carbon dioxide at 50 °C. *J. Supercrit. Fluids* **1990**, *3*, 51−65.

(25) Lim, J. S.; Park, J. Y.; Yoon, C. H.; Lee, Y. W.; Yoo, K. P. Cloud points of poly(L-lactide) in HCFC-22, HFC-23, HFC-32, HFC-125, HFC-143a, HFC-152a, HFC-227ea, dimethyl ether (DME), and HCFC-22 + CO_2 in the supercritical state. *J. Chem. Eng. Data* **2004**, *49*, 1622−1627.

(26) Eastoe, J.; Gold S. Self-assembly in green solvents. *Phys. Chem. Chem. Phys.* **2005**, *7*, 1352−1362.

(27) Olsen, S. A.; Tallman, D. E. Conductivity and voltammetry in liquid and supercritical halogenated solvents. *Anal. Chem.* **1996**, *68*, 2054−2061.

(28) Abbott, A. P.; Eardley, C. A.; Harper, J. C.; Hop, E. G. Electrochemical investigations in liquid and supercritical 1,1,1,2-tetrafluoroethane (HFC-134a) and difluoromethane (HFC-32). *J. Electroanal. Chem.* **1998**, *457*, 1−4.

(29) Tackson, K.; Fulton, J. L. Micriemulsions in supercritical hydrochlo-rofluorocarbons. *Langmuir* **1996**, *12*, 5289−5295.

(30) Butz, N.; Porte, C.; Courrier, H.; Krafft, M. P.; Vandamme, Th. F. Reverse water-in-fluorocarbon emulsions for use in pressurized metered-dose inhalers containing hydrofluoroalkane propellants. *Int. J. Pharm.* **2002**, *238*, 257−269.

(31) Eastoe, J.; Thorpe, A. M.; Eastone, J.; Dupont, A.; Heenan, R. K. Microemulsion formation in 1,1,1,2-tetrafluoroethane (134a). *Langmuir* **2003**, *19*, 8715−8720.

(32) Bush, D.; Echert, C. A.Prediction of solid−fluid equilibria in super-critical carbon dioxide using linear solvation energy relationships. *Fluid Phase Equilib.* **1998**, *150−151*, 479−492.

(33) Mendez, S. J.; Teja, A. S. The solubility of solids in supercritical fluids. *Fluid Phase Equilib.* **1999**, *158−160*, 501−510.

(34) Bartle, K. D.; Clifford, A. A.; Jafar, S. A. Solubilities of solids and liquids of low volatility in supercritical carbon dioxide. *J. Phys. Chem. Ref. Data* **1991**, *20*, 713−757.

(35) Hefter, G. T.; Tomkins, R. P. T. The experimental determination of solubilities. In *Solubility of Solids and Liquids in Supercritical Fluids*; Aim, K. K., Fermeglia, M., Eds.; John Wiley and Sons: London, 2003; Chapter 5.1, pp 493−556.

(36) Ozcan, A. S.; Clifford, A. A.; Bartle, K. D. Solubility of disperse dyes in supercritical carbon dioxide. *J. Chem. Eng. Data* **1997**, *42*, 590−592.

(37) Joung, S. N.; Yoo, K. Solubility of disperse anthraquinone and azo dyes in supercritical carbon dioxide at 313.15 K and from 10 to 25 MPa. *J. Chem. Eng. Data* **1998**, *43*, 9−12.

(38) Lee, J. W.; Min, J. M.; Bae, H. K. Solubility measurement of disperse dyes in supercritical carbon dioxide. *J. Chem. Eng. Data* **1999**, *44*, 684−687.

(39) Yamini, Y.; Bahramifar, N. Solubility of polycyclic aromatic hydro-carbons in supercritical carbon dioxide. *J. Chem. Eng. Data* **2000**, *45*, 53−56.

(40) Chrastil, J. Solubility of solids and liquids in supercritical gases. *J. Phys. Chem.* **1982**, *86*, 3016−3021.

(41) Peng, D.; Robinson, D. B. A new two-constant equation of state. *Ind. Eng. Chem. Fundam.* **1976**, *15*, 59−64.

(42) Liu, Z. T.; Erkey, C. Water in carbon dioxide microemulsions with fluorinated analogues of AOT. *Langmuir* **2001**, *17*, 274−277.

(43) Valderrama, J. O.; Alvarez, V. H. Phase equilibrium in supercritical CO_2 mixtures using a modified Kwak−Mansoori mixing rule. *AIChE J.* **2004**, *50*, 480−488.

(44) Angus, S.; Armstrong, B.; De Reuck, K. M. *IUPAC International Thermodynamic Tables of the Fluid State: Carbon Dioxide*; Butter-worth: London, 1971.

(45) Weng, W. L.; Che, J. T.; Lee, M. J. High-pressure vapor−liquid equilibria for mixtures containing a supercritical fluid. *Ind. Eng. Chem. Res.* **1994**, *33*, 1955.

(46) Yakoumis, J. V.; Vlachos, K. Kontogeorgis, G. M.; Coutsikos, P.; Kalospiros, N. S.; Tascios, D.; Kolisis, P. N. Application of the LCVM model to systems containing organic compounds and supercritical carbon dioxide. *J. Supercrit. Fluids* **1996**, *9*, 88.

(47) Vieira de Melo, S. A.; Costa, G.; Uller, A. M.; Pessoa, F. L. Modelling high-pressure vapor−liquid equilibrium of limonene, linalool and CO_2 systems. *J. Supercrit. Fluids* **1999**, *16*, 107.

(48) Caballero, A. C.; Hernandez, L. N.; Estevez, L. A. Calculation of interaction parameters for binary solid−SCF equilibria using several EoS and mixing rules. *J. Supercrit. Fluids* **1992**, *5*, 283.

(49) Valderrama, J. O.; Alvarez, V. H. Correct way of reporting results when modelling supercritical phase equilibria using equation of state. *Can. J. Chem. Eng.* **2005**, *83*, 578.

(50) Valderrama, J. O.; Alvarez, V. H. A Versatile thermodynamic consistency test for incomplete phase equilibrium data of high-pressure gas−liquid mixtures. *Fluid Phase Equilib.* **2004**, *226*, 149.